Subtraction of Compton-Scattered Photons in Single-Photon Emission Computerized Tomography

Bertil Axelsson, Peter Msaki, and Anders Israelsson

Karolinska Hospital and Karolinska Institute, Stockholm, Sweden

A technique for scatter correction in single photon emission computerized tomography (SPECT) is described. The method is based on "deconvolution" of scattered events from the measured profile data. The function defining the scatter distribution was determined from measurements with a line source in circular and rectangular water phantoms. The accuracy of the method was tested on a simple phantom simulating a SPECT investigation of the liver. The indicated ratio of the activity concentration in a photon-deficient area, 60 mm diameter in the "liver," relative to its surroundings, was 0.28/1 without scatter correction and 0.01/1 with the correction.

J Nucl Med 25: 490–494, 1984

The response of a position-sensitive detector, such as those used in conventional nuclear medicine imaging, is affected by scattered radiation. Scattered photons are of lower energy than the primary photons and could therefore in theory be eliminated by setting the baseline of the discriminator window at a photon energy equal to—or only slightly lower than—the energy of the primary photons. Currently, conventional and single photon emission computerized tomography (SPECT) nuclear medicine imaging systems use NaI(Tl) crystals, which limit their energy resolution to values typically in the range 10–15%. This means that although the energy of scattered photons is lower than the unscattered energy, some scatter counts do appear in the primary channels of the pulse-height analyzer. The limited energy resolution makes it virtually impossible to eliminate scattered photons even with the baseline of the energy window set at energies higher than the primary. In practice, however, the baseline must be set at lower energy than the energy of the primary photons, so that scattered radiation cannot be eliminated completely by this discrimination technique.

Received Aug. 8, 1983; revision accepted Nov. 16, 1983.

For reprints contact: Bertil Axelsson, Dept. of Hospital Physics, Karolinska Hospital, PO Box 60500, S-104 01 Stockholm, Sweden.

This imperfect discrimination against scattered radiation, which reduces both spatial resolution and signal-to-noise ratio, leads to degradation of image quality (*1–5*). Imperfect discrimination has also made it necessary to use attenuation coefficients in the range 0.09–0.14 cm^{-1} for attenuation correction (*6,7*). It is difficult to perform adequate attenuation correction because the selection of a particular value of attenuation coefficient depends, among other things, on the size of the source, which is usually not known.

Scatter-correction methods that have been used in conventional nuclear medicine imaging can, in principle, be used in SPECT. In general, the technique consists of establishing a scatter value or a scatter function that is subsequently subtracted from the measured data. In the past, information available for the scattered part of the energy spectrum has been used (*3,8,9*) to estimate the amount of scatter in the photopeak region, and thereby establish a scatter value for the correction.

A similar technique has recently been used in SPECT (*10*). The method increased the contrast between the original and the processed image by as much as 16%. The present work investigates the possibility of establishing a scatter function that could be applied in scatter correction according to the convolution technique that has been used for positron-emission tomography (*11*).

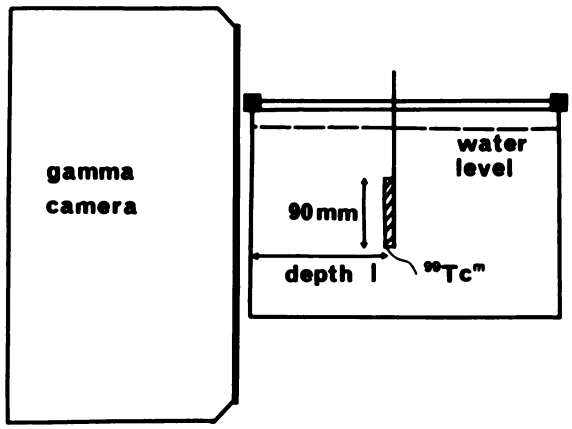

FIG. 1. Experimental set up for measurement of line spread function at different distances (l).

SCATTER-SUBTRACTION MODEL

The theory is based on the assumption that the measured projection data are a sum of primary and scattered photons and that the scatter contribution could be estimated from the measured data.

The scatter component S(x) at position x in the projection data is calculated by integral transformation of the projection data with a scatter-distribution function.

$$S(x) = \int_{-D}^{D} P(\tau) \times F(x - \tau)d\tau, \qquad (1)$$

where $P(\tau)$ denotes the projection data and $F(x - \tau)$ denotes the scatter amplitude at a distance $|x - \tau|$ from the position of the source. τ is a dummy variable, and 2*D is the width of the image field. The shape of the measured scatter distribution depends, of course, on the properties of the detector. Thus, the function $F(x - \tau)$ must be determined for the detection system to be used. To facilitate implementation of the scatter-subtraction technique in SPECT it is desirable that the scatter-distribution function should be practically independent of the position of the source within the investigated object.

MEASUREMENT OF SCATTER COMPONENT

The measurements were performed with a line source (diameter 2 mm, length 90 mm), filled with a solution of Tc-99m, in a water bath (height 280, width 280, and thickness 400 mm) in front of a gamma camera with a low energy general purpose collimator (Fig. 1). All measurements were corrected for decay due to differences in measurement time. A 22.5% discriminator window was centered on the photopeak.

In most applications of single photon emission computerized tomography, the mean of opposing views is used to obtain the projection data for the reconstruction. To simulate the results that would be obtained from this procedure with an object 300 mm in diameter (simulating the body), measurements were performed with the line source at various distances (l, Fig. 1) from 15 mm to 285 mm. The means of the measured data at 15 and 285, 50 and 250, and 100 and 200 mm were calculated and compared with the data measured with the source at 150 mm, which corresponds to the center of the investigated object. Both the arithmetic and geometric means were calculated. The results were evaluated as the number of counts/channel in a slice at the center of the line source. The results obtained using geometric mean are shown in Fig. 2. The shapes of the measured scatter distributions are quite similar for all distances (D) from the center except for D = 135 mm, which, as expected, will show less scattered radiation than the others due to the predominance of the small depth (15 mm) in the mean. Using the arithmetic mean, the magnitude at the peak of the line-spread function varies greatly with distance from the center. Therefore, the geometric mean was used in all subsequent evaluations.

Most patient contours are almost elliptical, which means that the clinical situation lies somewhere in between the rectangular object used in the measurements presented above and a cylinder. In order to study the influence on the scatter distribution of the shape of the object, measurements were made as described above, but starting with the line source at the center of a cylindrical water bath 300 mm in diameter. As can be seen from Fig. 3, these results differ little from those obtained from the rectangular phantom.

Measurements were also made with the line source moved, parallel to the collimator plane, to different positions (P) within the cylindrical water bath. Measure-

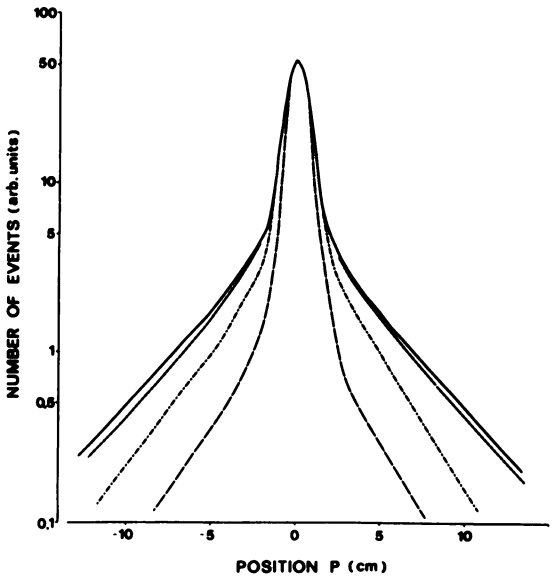

FIG. 2. Line spread functions (semilog.) from rectangular phantom, obtained using geometric mean of "opposing views." Distance D between line source and center of phantom: 0 mm (—), 50 mm (- - -), 100 mm (- · - ·), and 135 mm (— —).

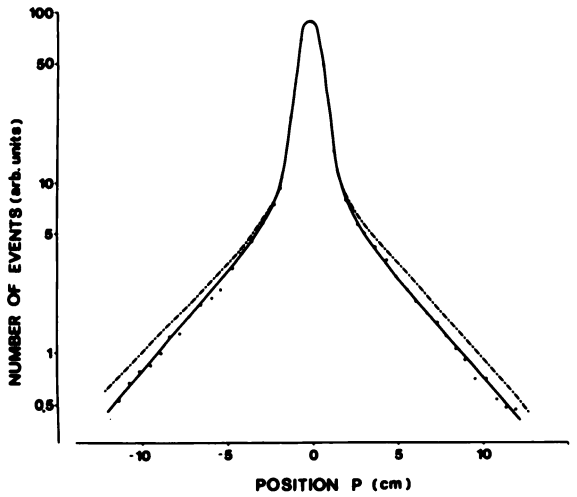

FIG. 3. Line spread functions (semilog.) obtained using rectangular (—) and circular (- · - ·) phantoms. Source is at center of phantom.

ments were made with the source at the center of the cylindrical water bath as well as at 50 mm, 100 mm, and 135 mm from the center. Due to the decreased attenuation close to the contour of the phantom, there is a slight increase in the amount of scattered radiation detected. This results in a change of the slope of the exponential function defining the "wings" of the measured distribution from 0.15 to 0.14. In a projected position outside the object, the number of registered counts/channel of course drops drastically due to lack of scattering material (Fig. 4).

CALCULATION OF SCATTER-DISTRIBUTION FUNCTION

The calculation of this function was made from the data obtained from the measurements with the line source in the rectangular water bath. The scatter function was considered to be defined by the linear "skirt" around the peak in Fig. 2, that is, as a monoexponential function.

$$F(x) = Ae^{-Bx}, \quad (2)$$

where x denotes distance, and the constant A is defined as the ratio between the number of counts/channel at the intersection of the two slopes defining the scatter distribution and the total number of counts in the measured line spread function. There are very small changes of this ratio with increasing distance from the center of the object (see Table 1). The difference, however, is marked for the 135-mm distance. The value of the constant B, which defines the slope of the scatter function (pixel^{-1}), shows small changes with distance from the center. From these data it appears reasonable to use the same values for A and B for all positions of the source, unless the source is very close to the contour of the object.

In determining which values should be used for the constants A and B in practical applications, we thought it appropriate to choose values that fit well if the source is positioned in between the center and the outer boundary of the investigated object, since—at least in a living body—the radiopharmaceutical is seldom con-

TABLE 1

Distance D from center (cm)	Scatter/total ratio	"Slope" of scatter function
0	0.032	0.15
5	0.035	0.17
10	0.035	0.23
13.5	0.011	0.18

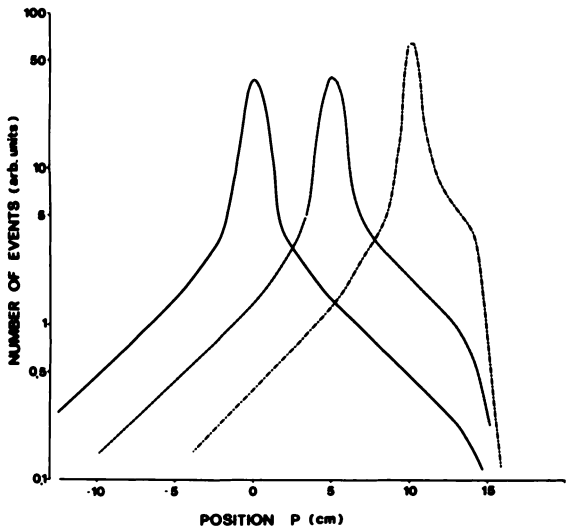

FIG. 4. Line spread functions (semilog.) from cylindrical phantom, obtained with line source at 0 mm (—), 50 mm (- - -), and 100 mm (- · - ·) from center of phantom.

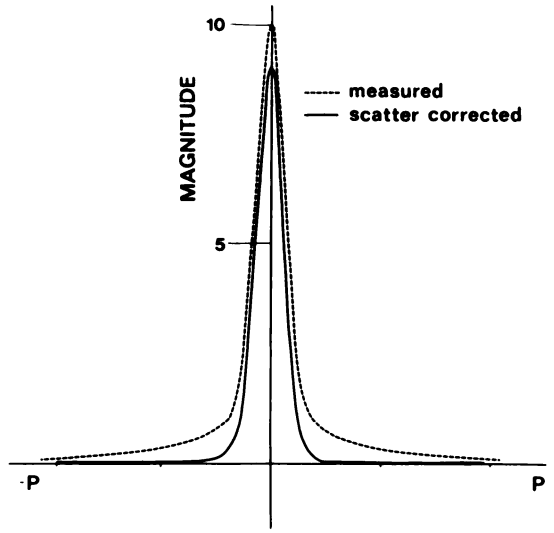

FIG. 5. Line spread functions (linear) obtained with line source at 50 mm from center of phantom: without scatter correction (- - -), and with scatter correction (—).

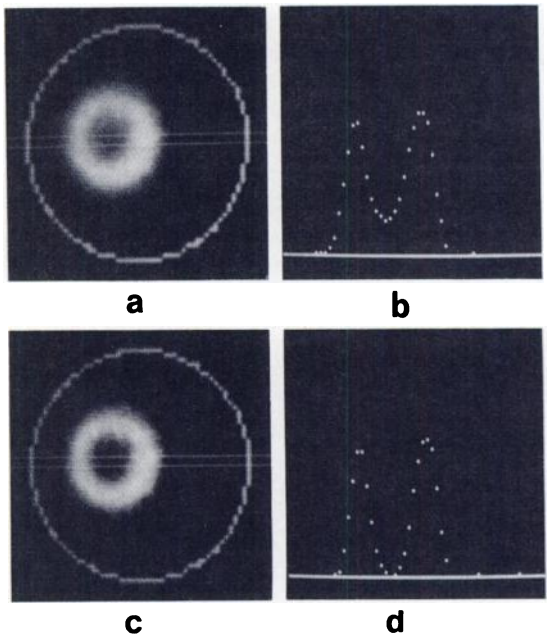

FIG. 6. Reconstructed SPECT images and linear profiles, obtained without scatter correction (a and b) and with it (c and d).

centrated close to the skin or at the center of the body. Thus the value for constant A was set at 0.035 and the value for constant B was chosen as the mean of the values for the 50- and 100-mm distances from center, yielding B = 0.20. The adequacy of these constants was tested on the measured line spread functions using the proposed technique for scatter subtraction. The results obtained using the data for the 50-mm distance from the center are shown in Fig. 5.

EXPERIMENTAL RESULTS

The effects of the scatter correction on SPECT scintigrams were tested in a situation roughly simulating an investigation of the liver. A cylindrical source (diameter 120 mm) containing a homogenous solution of Tc-99m was positioned inside the 300-mm cylinder, which was filled with water. The center of the source was 50 mm from the center of the cylinder. A cylinder 60 mm in diameter was positioned at the center of source. The activity in the 60-mm source was varied so that the ratio between the activity concentration in the 60-mm cylinder and that in the 120-mm cylinder ranged from 1:1 to 1:0. The axes of the cylinders were parallel to the axis of revolution of the SPECT camera.

The tomography system used has been described (*12*). The acquisitions were done at 64 angles and the images were reconstructed using geometric means of opposing views, together with the iterative attenuation-correction procedure presented by Larsson (*12*). All acquisition data were corrected for nonuniformity using the technique described by Axelsson et al. (*13*). Reconstructions were made both with and without scatter correction. In the latter case, a two-exponential function [$T(l) = 1.24\ e^{-0.14\,l} - 0.24\ e^{-0.32\,l}$], based on measured transmission, was used for attenuation correction, whereas a monoexponential function [$T(l) = e^{-0.15\,l}$] was used when scatter correction was performed before attenuation correction.

An example of the results obtained is shown in Fig. 6, which describes the case with zero activity in the 60-mm cylinder. There is a clear improvement of contrast using the scatter subtraction. The fraction of scattered radiation at the center of the 60-mm cylinder is decreased from 0.28 to 0.01.

Figure 7 shows the concentration ratios derived from the reconstructed images, with and without scatter correction, plotted against the true concentration ratio. The relation between true and measured concentration ratios is almost linear if the scatter correction is applied.

Emission tomography measurements were also made with the 300-mm diameter cylinder filled with a homogenous solution of Tc-99m. The 60-mm cylinder was positioned 50 mm from the center of the larger cylinder. The ratio between the activity concentration in the 60-mm and 300-mm cylinders was 0.5:1.0. The activity concentration ratio derived from the tomogram was changed from 0.65 to 0.41 using the scatter correction. The "overcorrection" results because the scatter-distribution function (as has been pointed out earlier) is not valid when the activity is close to the outer boundary of the investigated object.

DISCUSSION

The results presented imply that the proposed model for subtraction of scattered radiation could be of great value in SPECT investigations. The technique will im-

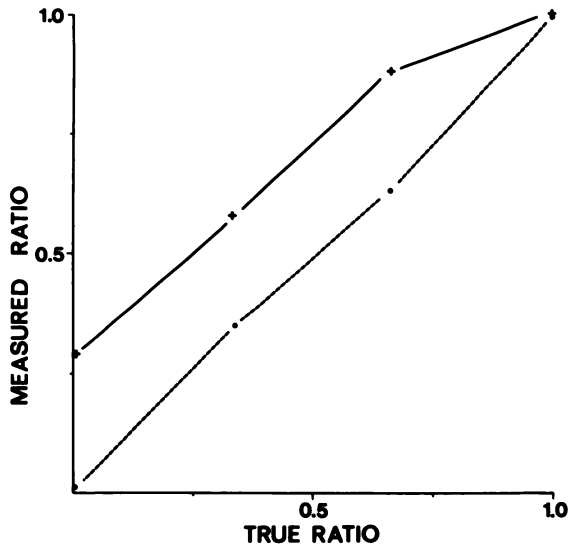

FIG. 7. True concentration ratio compared with concentration ratio measured from SPECT tomogram. Results obtained without scatter correction (—) and with (- - - -).

prove the contrast and probably the resolution of the reconstructed image. The noise level, however, will be increased. The performance of the method in other situations needs to be investigated further, as well as methods to optimize the parameters of the scatter-distribution function used. Furthermore, the impact of scatter subtraction on the attenuation correction must be considered if scatter subtraction is to be applied in a SPECT system.

REFERENCES

1. BECK JW, JASZCZAK RJ, COLEMAN RE, et al: Analysis of SPECT including scatter and attenuation using sophisticated Monte Carlo modeling methods. *IEEE Trans Nucl Sci NS-29*, No 1: 506-511, 1982
2. PANG SL, GENNA S: The effect of Compton scattered photons on emission computerized transaxial tomography. *IEEE Trans Nucl Sci NS-26*, No 2: 2772-2774, 1979
3. BECK RN, SCHUH MW, COHEN TD, et al: Effects of scattered radiation on scintillation detector response. In *Medical Radioisotope Scintigraphy*. Vol 1, Vienna, IAEA, 1969, pp 595-616
4. ERHARDT JC, OBERLEY LW, LENSINK SL: Effect of scattering medium on gamma-ray imaging. *J Nucl Med* 15:943-948, 1974
5. SHERMAN IS, STRAUSS MG, BRENNER R: Compton scatter in Germanium and its effect on imaging with gamma-ray position-sensitive detectors. *IEEE Trans Nucl Sci NS-25*, No 1: 665-675, 1974
6. MSAKI P, LARSSON SA: Determination of scatter fractions and effective linear attenuation coefficients from measurements of $^{99}Tc^{m}$ plane sources in water. Internal report 1983-01, Department of Radiation Physics, Karolinska Institute, Stockholm, Sweden
7. MACEY DJ, MARSHALL R: Absolute quantitation of radiotracer uptake in the lungs using a gamma camera. *J Nucl Med* 23:731-735, 1982
8. BLOCK P, SANDERS T: Reduction of the effects of scattered radiation on a sodium iodide imaging system. *J Nucl Med* 14:67-72, 1973
9. WAGGETT DJ, WILSON BC: Improvement of scanner performance by subtraction of Compton scattering using multiple energy windows. *Br J Radiol* 51:1004-1010, 1978
10. JASZCZAK RJ, COLEMAN RE, GREER KL: The subtraction of scattered events from SPECT photopeak events. *J Nucl Med* 24:P82, 1983 (abst)
11. BERGSTRÖM M, ERIKSSON L, BOHM C, et al: Correction for scattered radiation in a ring detector positron camera by integral transformation of the projections. *J Comput Assist Tomogr* 7:42-50, 1983
12. LARSSON SA: Gamma camera emission tomography, development and properties of a multi-sectional emission computed tomography system. *Acta Radiologica* (Suppl. 363): 1980
13. AXELSSON B, ISRAELSSON A, LARSSON SA: A method for correction of gamma camera non-uniformity in single-photon emission computed tomography. Gasteiner Internationales Symposium 1982. In *Radioaktive Isotope in Klinik und Forshung*. Vol. 15, No. 2, Höfer R, Bergmann H, eds. 1982, pp 519-527